



**HAL**  
open science

## Experimental testing of arches with rectangular hollow sections

Cyril Douthe, Konstantinos Adamakos, Charalampos Gantes, Xenophon Lignos

► **To cite this version:**

Cyril Douthe, Konstantinos Adamakos, Charalampos Gantes, Xenophon Lignos. Experimental testing of arches with rectangular hollow sections. Eurosteel 2011, Aug 2011, Hungary. pp 2181-2186. hal-00852347

**HAL Id: hal-00852347**

**<https://hal.science/hal-00852347>**

Submitted on 20 Aug 2013

**HAL** is a multi-disciplinary open access archive for the deposit and dissemination of scientific research documents, whether they are published or not. The documents may come from teaching and research institutions in France or abroad, or from public or private research centers.

L'archive ouverte pluridisciplinaire **HAL**, est destinée au dépôt et à la diffusion de documents scientifiques de niveau recherche, publiés ou non, émanant des établissements d'enseignement et de recherche français ou étrangers, des laboratoires publics ou privés.

## EXPERIMENTAL TESTING OF ARCHES WITH RECTANGULAR HOLLOW SECTIONS

C. Douthe<sup>(1)</sup>, K. Adamakos<sup>(2)</sup>, C.J. Gantes<sup>(2)</sup> and X. Lignos<sup>(2)</sup>

<sup>(1)</sup> Université Paris-Est, France

<sup>(2)</sup> National Technical University of Athens, Greece

### 1 OBJECTIVES OF THE EXPERIMENT

The aim of the present paper is the experimental investigation of the relative importance of the parameters governing the design of steel arches. What first excited our curiosity were two sections of the specialist design guide edited by the Steel Construction Institute entitled: “Design of curved Steel” [1] which pointed out two specificities of curved members that may have a noticeable influence on the behaviour and stability of steel arches.

The first one is the fabrication process of the curved members and more precisely the cold curving process which is the cheapest and the more common way to produce curved members by bending of straight members. The non-reversible deformations introduced by this process are associated with self-equilibrated stresses or residual stresses locked in the section (see figure 1 for a typical distribution). Actually, the presence of residual stresses is not specific to curved members. Their influence on the behaviour of the hot-rolled or cold formed straight members has been abundantly studied, quantified [2] and incorporated in the design methodology and all standards for steel construction [3, 4]. Yet the way in which residual stresses influence the behaviour depends on their distribution in the cross section which is very different in the case of curved members than in straight members. Indeed figure 1 shows that, for cold curving, this distribution is non-symmetrical through the section height and has significant magnitude in the web (after [1]). It is thus expected that this asymmetry will lead to a different behaviour depending on the sign of the bending moment and that the high level of stresses in the web will cause early yielding under normal forces.

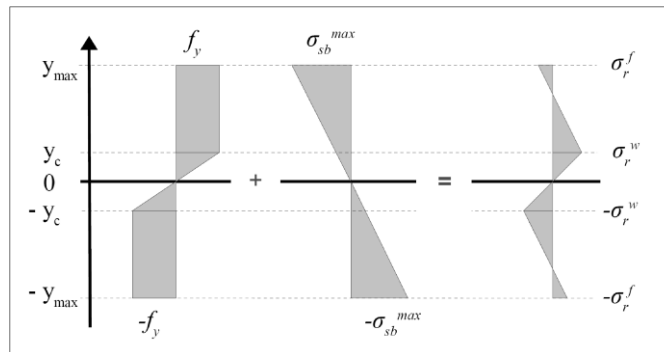


Figure 1: Curving stresses, elastic spring-back and residual stresses due to cold curving

The second one is the transverse bending stresses. These stresses do not appear in straight members because they result from the curvature, as illustrated on figure 2 which shows a curved member with rectangular hollow section subjected to bending. The bending of the cross-section induces normal compression stresses in the upper flange and normal tension stresses in the lower flange. These stresses act perpendicularly to the cross section, so that they are not equal and opposite, and by then not self-equilibrated. They induce radial pressures which are resisted first by transverse bending of the flanges and then by normal stresses in the webs. These transverse stresses have already been analysed and quantified [1, 5, 6].

However, like for the residual stresses due to cold curving, the influence of these stresses on the elasto-plastic behaviour relatively to other design parameters such as geometric imperfections or geometric non-linearities is not clear and that is why it will be investigated here.

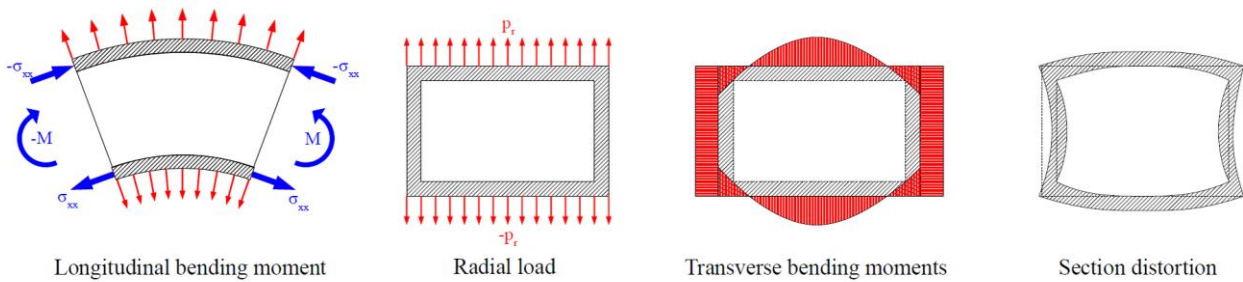


Figure 2: Radial pressure due to transverse bending in curved rectangular hollow sections.

## 2 DESCRIPTION OF THE EXPERIMENTAL SETTING

### 2.1 Constraints of the experiment

It has been seen in the first section that the curving process induces a non-symmetrical distribution of residual stresses through the cross-section and influences the behaviour of the curved member in a different way if the applied bending moment “opens” or “closes” the arch. The experimental protocol should thus allow for both directions of bending moments. The first section also emphasised that bending induces transverse bending stresses and distortion effects which are proportional to the curvature, to the width of the flanges and to the inverse of the thickness. The tested specimen should thus be chosen with large curvature and flanges as large and as thin as possible. Beside, the laboratory facility had its own constrains: the dimensions of the testing frame and the capacity and the stroke of the available hydraulic press. These restrictions translate into a maximum span of the arch of 4.725 m, a maximum height of 1.10 m below the press and loads preferably not exceeding 50 kN.

All these constrains lead to a set of twelve experiments on hinged circular arches loaded by a concentrated force at crown (figure 3). This set comprises six compression tests inducing opening bending moments at crown and six tension tests inducing closing bending moments at crown. Two different radii of curvature were investigated:  $R = 3.71$  m and  $R = 4.10$  m, and the corresponding arches were designated as high arches and low arches, respectively.

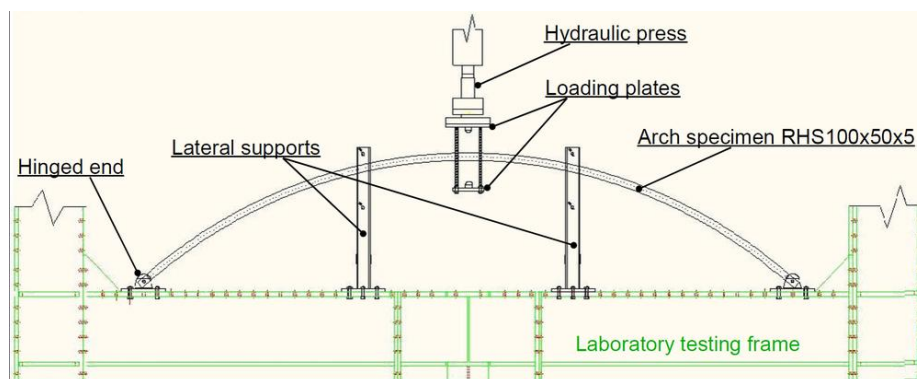


Figure 3: Scheme of the experimental setting.

### 2.2 The arches and auxiliary elements

A common cross-section was chosen for all specimens: a rectangular hollow section RHS 100x50x5, made of S355 quality steel. The members were curved along their weak axis to give them higher out-of-plane stiffness and to allow working with lower loads. Despite those precautions, numerical simulations showed that the first out-of-plane buckling load was relatively close to the ultimate load of the arches. Lateral supports were thus added at the thirds of the span to provide additional out-of-plane protection. The inner face of the supports was covered by Teflon™ foils to reduce friction between the arch and the support. At their ends the arches were hinged to the

laboratory testing frame and reinforced locally by 10 mm thick plates to avoid yielding in the vicinity of the pivot axes. The loading plate was a 30 mm thick plate, on which half of a cylinder was welded. In the compression tests configuration, it was fixed directly to the press by bolts whereas in the tension tests configuration, it was inverted and attached to the press through four shanks. All auxiliary elements were designed according to EC3, verifying that their deformations would be at least one order of magnitude lower than those of the arches.

### **2.3 The measuring devices**

The hydraulic press, which is displacement controlled, includes a load cell (which gives the applied load) and a displacement cell corresponding to the imposed displacement at crown. The deflected shape of the arch was also assessed by an inclined LVDT on each side, perpendicularly to the arch (their position was selected on the basis of a linear static analysis and corresponds to the point of maximal deflection in the opposite direction of that at crown) and three LVDTs located at 150 mm left of the crown. These three LVDTs were placed in a vertical plane and used to measure local torsion or rotation and distortion through relative displacement of the central LVDT and the two others. Four strain gages, two 90° tee rosettes and two linear gages, were set on each specimen in a vertical plane situated at 150 mm on the right of the crown. The rosettes were located in the middle of the top and bottom flanges and oriented to measure longitudinal and transverse strains. The linear gages were located on the top flange on the limit of the plane surface and oriented to measure longitudinal strains and assess the uniformity of the stress distribution in the top flanges.

### **2.4 Remarks on imperfections**

Imperfections are inevitable when materialising an experimental setting and some adjustments have to be done. Indeed, the curving process is not perfect and the in-plane curvature is not uniform. A set of six measurements for each specimen was thus conducted to evaluate the initial span of the arch (the high arches were generally 8 mm larger and the low arches 15 mm shorter) and the defaults of symmetry (a maximum difference of approximately 5 mm between the heights of the first and second half of the arch was measured on each specimen). As the span does not fit within the position of the hinges, a temporary sliding system had to be installed to open or close the arch and to bring the hinge to the right position before it was fixed. This system was easy to manage but introduced a prestress into the arch which was calculated from the measurements of the initial span.

## **3 ANALYSIS OF EXPERIMENTAL RESULTS**

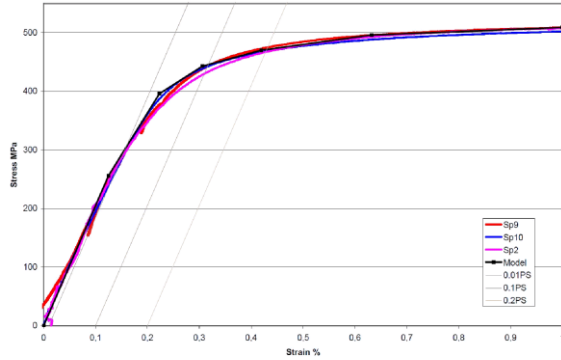
### **3.1 Material tests**

In parallel to the experiment on arches, material tests were conducted to investigate the material behaviour and to define a model of steel to be used in the numerical simulations. To this end, small pieces of the straight members were removed at the ends before their curving. Coupons or tension strip specimens were then cut off the tubes flanges and set in the usual “bow tie” form following DIN standards for specimen geometry. Three coupons from three different arches (specimen 2, 9 and 10) were tested and the corresponding results are presented in figure 4 and summarized in table 1. As the results were consistent, no further tests were required.

The main characteristics of the material were determined progressively starting from the Young modulus, which was found close to 205 GPa, as expected. The proportional limit and the yield stress were then evaluated following the usual convention, namely they correspond to a plastic strain of 0.01 % and 0.2 % respectively. The ultimate tensile stress and strain were obtained graphically from the complete stress-strain curve. These latter values confirmed that the quality of the steel was S355. However, it is remarkable that the transition between the elastic and the plastic domains is very smooth and starts very early. This is a consequence of the forming process of the rectangular hollow section which caused significant hardening of the material and high residual stresses longitudinally and transversally [2].

From the material tests, it is concluded that it would have been erroneous to use the theoretical bilinear stress-strain law of S355 to model the behaviour of the chosen section. The multi-linear

model shown in figure 4 was hence adopted for the numerical modelling. A simplified bilinear elastic-perfectly plastic model was also used for the analytic study: based on the fact that, during curving, the plastic strain in the flanges exceeded 0.6 %, one can consider that, after curving the yield stress is 505 MPa. A side conclusion from these material tests was that one should be very careful when designing structures with such hollow sections, especially when stresses approach the theoretical yield stress.



Proportional limit (MPa) ( $\epsilon_p=0.01\%$ )	$271 \pm 13$
Yield stress $f_y$ (MPa) ( $\epsilon_p=0.2\%$ )	$470 \pm 4$
Ultimate tensile stress $\sigma_u$ (MPa)	$544 \pm 9$
Ultimate tensile strain $\epsilon_u$ (%)	$10.3 \pm 0.3$

Figure 4: Behaviour of tensile strips and multi-linear model. Table 1: Material main characteristics.

### 3.2 Behaviour of the arches

As mentioned above, two different types of tests were conducted: compression and tension tests on two different geometries of arches: high and low arches. All tests were displacement controlled and followed the same protocol: a first loading step up to 20 mm, then an unloading step back to 10 mm and then a second loading step until 80 mm for tension tests and 95 mm for compression tests. The small cycle between 10 mm and 20 mm (within the elastic range) does not go back until the initial position of the press (0 mm) in order to remain in the domain where the clearances do not influence the tests. Indeed, the high arches had too large spans and thus leaned on the external side of the hinges; yet to resist the forces during tension tests, the arches have to lean on the internal side of the hinges and thus, when starting applying the load, the arches slide within the support to recapture all clearances (approximately 3 mm on each side). Such sliding is evident on the typical displacement-load curves presented in figure 5a for the tension tests on a high arch. Figure 5b represents such a curve for a compression test on a high arch.

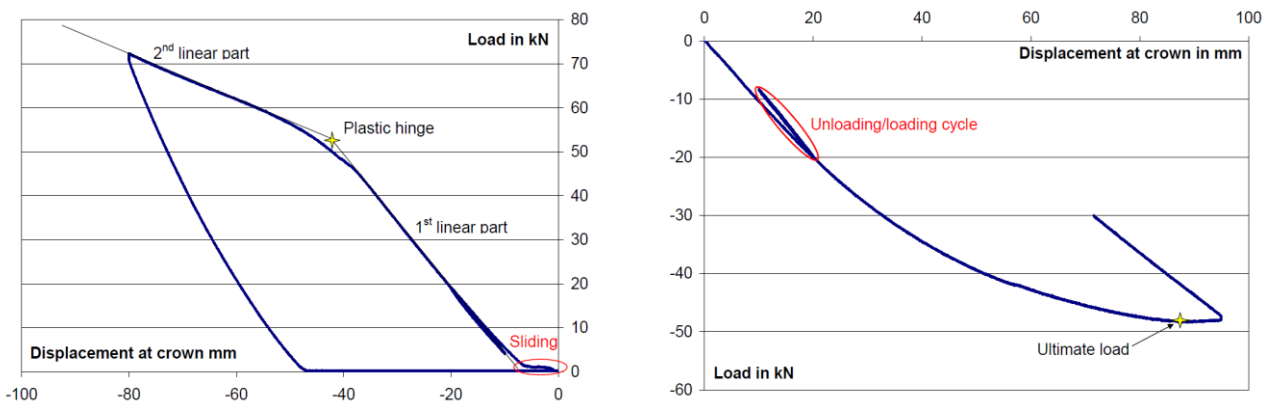


Figure 5: Typical behaviour of arches, a) under tension, b) under compression.

The two curves are very different. The arch under tension (figure 5a) presents a clear linear part until 45 kN, then its stiffness gradually diminishes to reach another linear part after 55 kN as predicted by a linear analytical model with a single plastic hinge at crown. On the contrary, the arch under compression (figure 5b) does not exhibit any linear part, even for low load and reaches its ultimate load by progressive softening. These differences are attributed to the sensitivity of the two configurations to geometric non-linearities. When compressed, the arch deforms in a way that the displacements and the associated second order forces induce additional deformations, it behaves

like a softening structure. When tensed, the arch deforms in a way that brings it closer to the funicular geometry associated with a concentrated load at crown and consequently it behaves as a stiffening structure; the deformations remain very small and the hypothesis of linear elasticity is verified until and even after the forming of the plastic hinge at crown.

Following these qualitative observations more quantitative aspects have been addressed. For all the tests, different magnitudes were evaluated and calculated within the load cycles which exhibit linear and homogeneous properties, namely:

- the global stiffness (load/displacement at crown) in all linear parts ( $K_1$  and  $K_2$ ),
- the ultimate load  $P^{ult}$  (maximum load in compression test),
- the load at which the plastic hinge forms  $P^{pl}$  (by interpolation of the two linear parts in tension tests),
- the lateral stiffness (load/displacement on the side  $K_{lat}$ ) which assesses also the symmetry of the test by comparison of the two sides,
- the ratio between transverse strain and longitudinal strain ( $\epsilon_{xx}/\epsilon_{yy}$ ).

In general, the different experiments gave homogeneous results and the discrepancy of the various measures between the three identical tests was often smaller than 5 %, which can reasonably be attributed to the various geometric imperfections of the arches. No significant asymmetry or rotation was noticed. Most comparisons between experimental and numerical results conducted with ADINA™ showed good agreement except for the strain gages in compression tests (table 2). The real arches are slightly softer than their model, especially the high arches.

		Tension tests				Compression tests		
		$K_1$	$P^{pl}$	$K_2$	$K_{lat}$	$K_1$	$P^{ult}$	$K_{lat}$
		kN/mm	kN	kN/mm	kN/mm	kN/mm	kN	kN/mm
High arch	Exp.	1.5	54	0.51	3.8	1.2	48.3	3.2
	Num.	1.7	62	0.39	2.9	1.3	48.9	2.6
Low arch	Exp.	1.7	61	0.65	4.1	1.2	47.9	3.4
	Num.	1.8	64	0.41	3.2	1.3	48.7	2.8

Table 2: Characteristic values for stiffness's and characteristic loads.

### 3.3 Influence of the curving process

The influence of the curving process should have been investigated through the comparison between the elasto-plastic behaviour in compression and in tension. Nevertheless, it has just been seen that the behaviour under compression is very much influenced by the geometric non-linearities on the contrary to the behaviour under tension, so that experimentally no direct comparison of the yield points could be done. It is, however, clear that the curving process influences the behaviour of the arches. During forming, the section undergoes considerable plastic deformations which cause hardening of the material and increase its yield point. From the material tests, one deduces that the yield point in the flanges is over 500 MPa after curving. This is confirmed by the ultimate load in compression and the load at which the plastic hinge develops in tension for which analytical and numerical models show that necessarily the yield stress is between 500 and 510 MPa.

### 3.4 Transverse bending stresses

The two 90° tee rosettes allowed clear experimental evaluation of transverse bending stresses. The results of the measurements are shown in table 3. The ratios  $(\epsilon_{yy} - \nu \epsilon_{xx})/\epsilon_{xx}$  shown in this table are calculated at the very beginning of the test to avoid the effects of geometric non-linearities. It is noticed here that the longitudinal strain  $\epsilon_{xx}$  comprises also a contribution of the normal force which is hence included in the analytical model. The similarity between experimental values in tension and in compression is remarkable, so that these values can be considered as characteristic of the

magnitude of transverse stresses in RHS100x50x5. The values are slightly higher in tension but as tension tests cause bending moments in the same direction as the curving moments, the distortion of the section might be increased by initial deformations. The difference between the upper and lower flange might be explained partly by the influence of normal forces and partly by the fact that there is a weld in the middle of the lower flange.

	Tension tests		Compression tests	
	Upper	Lower	Upper	Lower
Experimentally	-0.124±0.004	0.165±0.005	-0.116±0.005	0.16±0.02
Analytical	-0.144	0.166	-0.144	0.166

Table 3: Relative magnitude of transverse bending stresses for high arches.

#### 4 CONCLUSIONS

First of all, these experimental tests allow the verification of some important general features of the behaviour of arches: the influence of geometrical imperfections, that of geometrical non-linearities and that of the stiffness of the supports and of the necessary clearances. They have also helped point out that working with cold formed members such as rectangular hollow sections means working with steel members with complex hardening elasto-plastic behaviour. Concerning the two specific phenomena focused in this article, the measurements of transverse strains clearly validated the analytical model, its influence on the overall plastic behaviour does however not seem so significant. The influence of the curving process and the asymmetry of the behaviour induced by the residual stresses could not be quantified as planned, mainly because of the non-linear behaviour of the arch under compression. The influence of the curving process on the material law was however evidenced and should be considered when considering plastic design of curved members.

#### 5 ACKNOWLEDGMENT

The authors gratefully acknowledge the support of the European Community under a Marie Curie Intra-European Fellowship for Career Development (Grant agreement number 235196).

#### REFERENCES

- [1] Steel Construction Institute, Design of Curved Steel, 2001, 111 pages.
- [2] Key P.W. & Hancock G.J., A theoretical investigation of the column behaviour of cold-formed square hollow sections, *Thin-Walled Structures* 16 (1993), 31-64.
- [3] ECCS Committee 8, *Manual on Stability of Steel Structures*, 2<sup>nd</sup> edition, n°22, 1976, 26 pages.
- [4] Galambos T.V., Chapter three: Centrally loaded Columns, *Guide to Stability Design for Metal Structures*, John Wiley & Sons Inc, 5<sup>th</sup> edition (1998), 33-45.
- [5] Cook R.D. & Young W.C., Chapter 10: Curved beams, in *Advanced Mechanics of Materials*, eds Macmillan (1985), 411-442.
- [6] Timoshenko S., Bending stresses in curved tubes of rectangular cross section, *Transactions of the ASME*, vol. 45 (1923), 135-140.